Third-order optical spectroscopy of polythiophene

Myoungsik Cha, William E. Torruellas, Sui H. Yuan, and George I. Stegeman

Center for Research and Education in Optics and Lasers, University of Central Florida, 12424 Research Parkway, Orlando, Florida 32826

Mario Leclerc

Département de Chemie, Faculté des Arts et Sciences, Université de Montréal, C.P. 6128, Succursale A, Montréal, Québec H3C 3A7, Canada

Received August 4, 1994

Tunable third-harmonic generation and nondegenerate four-wave mixing experiments were performed on polythiophene thin films to produce six independent nonlinear-optical spectra. An essential states model consisting of three electronic excited states has been compared with the spectra. Inclusion of a Raman state could improve the fit to two of the spectra.

1. INTRODUCTION

Polyacetylenes and polydiacetylenes have been the most extensively studied π-electron conjugated polymers because of their large cubic nonlinearities and the availability of samples in crystalline and thin-film forms. A continuing problem has been to develop new kinds of conjugated polymer with enhanced nonlinearities and stability.[1] Polythiophenes belong to a relatively new class of π-electron conjugated polymers that show large electronic $\chi^{(3)}$, comparable with those of polydiacetylenes.[2–5] The molecular structure of polythiophenes is shown in Fig. 1. Like polyacetylenes and polydiacetylenes they also possess the C_{2h} point group symmetry. The π electrons are delocalized along the main chain, providing high electronic nonlinearity. Because this main chain alone is insoluble, side chains are added to solve this problem. Although adding a longer side chain usually gives better solubility, it results in a reduced linear- and nonlinear-optical response owing to the volume dilution of the optically active main chain in the sample.[6] In the current experiments thin films of poly(3-tetradecyl-thiophene) (PT14) were used.

Tunable third-harmonic generation (THG) and degenerate four-wave mixing experiments have been performed to estimate the cubic susceptibilities of polythiophenes.[2–5,7–9] Recently the $\chi^{(3)}(-3\omega;\omega,\omega,\omega)$ spectra were measured and interpreted successfully by an empirical four-level model consisting of the ground state, one B_u, and two A_g excited states that possess odd and even parities, respectively.[10] The same spectra were equally well interpreted by another four-level model that incorporates two B_u and one A_g excited state derived from a calculation based on an extended Hubbard model.[11] In both cases the two-photon states are not clearly located because of the inherent characteristics of THG in which the 2ω resonance either lies outside the experimental wavelength range or interferes with the 3ω resonance. Furthermore, there is no clear signature for identifying one-photon (B_u) versus two-photon (A_g) states. Obviously one needs other complimentary experiments such as two-photon absorption (TPA) and nondegenerate four-wave mixing (NDFWM) in the frequency range of interest to probe different admixtures of the states' contributions to $\chi^{(3)}$.

In this paper the experimental THG and NDFWM spectra are presented for the polythiophene, poly(3-tetradecylthiophene) (PT14). The four-level model that had been used previously to fit the THG data is tested against extended THG data as well as new NDFWM data, and the limits of this model are discussed.

2. SAMPLE PREPARATION AND LINEAR PROPERTIES

The details of the syntheses of polythiophenes are described elsewhere.[12,13] In brief, PT14 polymer was dissolved in chloroform (50 mg/2 mL) and mixed in an ultrasonic bath at room temperature for 1 h. The solution was then filtered and spin coated at 2000–5000 rpm onto a fused-silica substrate, 2.54 cm × 2.54 cm and 6 mm thick. The spin-coated films had thicknesses of 100–500 nm as measured with a profilometer (Tencor Alpha Step).

The linear absorption spectrum was taken with a computer-controlled Perkin-Elmer 330 spectrophotometer and is shown in Fig. 2. The absorption peak near 500 nm (2.5 eV) is associated with the electronic transition from the ground state ($1A_g$) to the first one-photon excitonic state ($1B_u$). No significant absorption is observed for $\lambda > 650$ nm. The same absorption measurement was repeated on a sample from the same batch of material after all the nonlinear experiments had been done to verify that the polymer film had not degraded in the atmosphere over the duration of the nonlinear-optical experiments.

0740-3224/95/050882-07$06.00

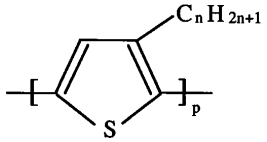

Fig. 1. Molecular structure of PT14: $n = 14$.

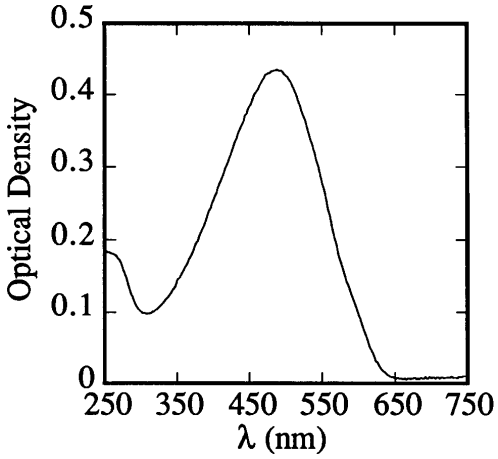

Fig. 2. Linear absorption spectrum for PT14. Film thickness 115 nm.

3. THIRD-HARMONIC GENERATION AND NONDEGENERATE FOUR-WAVE MIXING

A complement to the linear absorption spectrum is the TPA spectrum. The latter gives the most direct information about two-photon states because the TPA coefficient is proportional to $\mathrm{Im}[\chi^{(3)}(-\omega;\omega,-\omega,\omega)]$, which contains only one- and two-photon resonances. However, direct TPA measurements require a thick sample of good optical quality, which could not be obtained in the present case. In addition, such degenerate measurements need ultrashort laser pulses to isolate pure TPA from possible higher-order or excited-state absorptions. Because THG and NDFWM are nondegenerate, nanosecond laser pulses can be used without being affected by the excited-state absorption. These techniques are also less susceptible to higher-order effects because one can use smaller intensities than in the degenerate case. (The signals are spectroscopically separated from the fundamental beams.) Schematic diagrams of these third-order processes are presented in Fig. 3. The THG and NDFWM techniques were thus utilized to measure the corresponding cubic susceptibilities, probing the associated electronic excited structure of polythiophene. Higher-order effects, including those that are due to excited-state populations, are negligible under the current experimental conditions. By repeating the same experiments with different input pulse energies we verified that no intensity or fluence dependence contributed to the experimental results presented here. When excited-state populations can be neglected, the dominant terms in the sum-over-states expansion for THG are

$$\frac{\mu_{gu}\mu_{ug'}\mu_{g'u'}\mu_{u'g}}{(\Omega_{gu}-3\omega)(\Omega_{gg'}-2\omega)(\Omega_{gu'}-\omega)} - \frac{|\mu_{gu}\mu_{gu'}|^2}{(\Omega_{gu}-3\omega)(\Omega_{gu}-\omega)(\Omega_{gu'}-\omega)}, \quad (1)$$

whereas for NDFWM with output at $2\omega_1-\omega_2$ $(=\omega_3)$ the dominant terms are

$$\frac{|\mu_{gu}\mu_{gu'}|^2}{(\Omega_{gu}-\omega_3)(\Omega_{gu}-\omega_1)(\Omega_{gu'}-\omega_1)} - \frac{|\mu_{gu}\mu_{gu'}|}{(\Omega_{gu}-\omega_1)(\Omega_{gu}^{*}-\omega_2)(\Omega_{gu'}-\omega_1)}, \quad (2)$$

$$\frac{\mu_{gu}\mu_{ug'}\mu_{g'u'}\mu_{u'g}}{(\Omega_{gu}-\omega_3)(\Omega_{gg'}-2\omega_1)(\Omega_{gu'}-\omega_1)} + \frac{\mu_{gu}\mu_{ug'}\mu_{g'u'}\mu_{u'g}}{(\Omega_{gu}^{*}-\omega_2)(\Omega_{gg'}-2\omega_1)(\Omega_{gu'}-\omega_1)}. \quad (3)$$

Here the subscript g signifies the ground state, and u and g' indicate one- and two-photon excited states, respectively.[14] Ω_{k0} is the complex angular frequency associated with the excited state k defined by

$$\Omega_{k0} = E_{k0}/\hbar - i\Gamma_{k0}/2, \quad (4)$$

where E_{k0} is the energy difference between the state k and the ground state (0) and Γ_{k0} is the associated inverse radiative lifetime in the case of homogeneous broadening. Then Γ_{k0} is the full width at half-maximum of the Lorentzian line shape. μ_{lm} is the transition dipole moment between the states l and m. In both THG and NDFWM the positive contribution is due to the presence of a two-photon active oscillator, whereas the negative contribution can be interpreted as the asymptotic tail of a one-photon active oscillator acting as a classical saturable absorber. Because the contributions of the different transitions to the third-order susceptibility $\chi^{(3)}$ change with different frequency inputs and outputs, theoretical predictions can be tested with several nonlinear spectroscopic experiments. In this case, THG and NDFWM with two different fixed frequencies ω_2 were used ($\lambda_2 = 1064$ nm and $\lambda_2 = 1907$ nm).

For THG and NDFWM experiments the Maker fringe technique is adopted to yield both the magnitude and

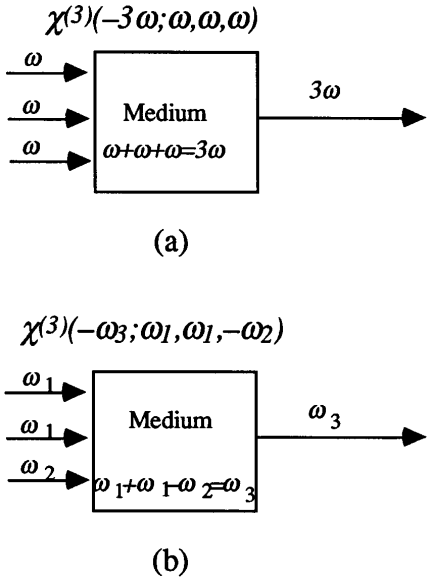

Fig. 3. Schematic diagrams of (a) THG and (b) NDFWM processes.

the phase of $\chi^{(3)}$ for the polythiophene thin film. Maker fringes, $I_{3\omega}(\theta)$, are the output (THG or NDFWM) signal intensities (or pulse energies) obtained as a function of the incident angle from a thin film deposited upon a substrate.[15] For THG a third-harmonic wave is generated from every small volume in a medium encountered in the path of the fundamental beams, and the sum of these generated fields at the exit plane determines the intensity of the third-harmonic wave detected outside the sample. One can define the coherence length associated with the THG process as

$$l_c = \pi/\Delta k\,, \tag{5}$$

where the wave-vector mismatch is given by

$$\Delta k = k(3\omega) - 3k(\omega) = \frac{3\omega}{c}\,[n(3\omega) - n(\omega)] \tag{6}$$

and $n(\omega)$ and $n(3\omega)$ are (linear) refractive indices at the fundamental and third-harmonic wavelengths, respectively. A maximum or minimum in the Maker fringe is obtained when the optical path has changed by Δl, which is equal to the coherence length. NDFWM Maker fringes occur essentially in the same way as those for THG, except that the wave-vector mismatch condition is given as follows in the case of collinear propagation of the two fundamental beams:

$$\begin{aligned}\Delta k &= k(\omega_3) - [2k(\omega_1) - k(\omega_2)] \\ &= \frac{\omega_3}{c}\,n(\omega_3) - \left[\frac{2\omega_1}{c}\,n(\omega_1) - \frac{\omega_2}{c}\,n(\omega_2)\right],\end{aligned} \tag{7}$$

where $\omega_3 = 2\omega_1 - \omega_2$. Both THG and NDFWM output signals can be calculated starting from the wave equation for the optical frequencies.[16] Multireflections at the interfaces also can be included by use of a matrix approach.[17,18] A typical sample is composed of a fused-silica substrate with an organic thin film coated onto it. Because both film and substrate generate signals, the contribution from the film is obtained from the combined Maker fringe data.[15,17] The film thickness is much less than one coherence length; thus it alone does not give any additional modulation to the Maker fringe but adds almost a constant (angle-independent) signal to the full contrast fringe signal from the substrate. Coherence lengths of fused silica are 2–18 μm for THG and 22–1800 μm for NDFWM in the wavelength range of interest. Thus the overall Maker fringe from the sample (film + substrate) will be modulated with some dc level that contains information on the magnitude of $\chi^{(3)}$ of the film. The phase information about $\chi^{(3)}$ is contained in a shift of the fringe patterns between the coated sample (film + substrate) and the substrate only. Two sets of Maker fringes, one for the substrate with film and the other for the substrate alone (after the film is removed), are taken without any change in the experimental conditions at each fundamental wavelength. Typical Maker fringe data are shown in Fig. 4. By fitting these two sets of data, using the Maker fringe analysis discussed above, one obtains the complex $\chi^{(3)}$ of the organic film with reference to that of the fused-silica substrate. The linear data such as the thickness and dispersion of the absorption coefficient and the refractive index for each layer are necessary as input parameters for THG or NDFWM Maker fringe fitting.

UV-quality fused silica is chosen as the substrate because it has very little absorption in the spectral regions of both the fundamental and the harmonic waves (700–1900 and 230–630 nm, respectively). Z-scan measurements of α_2 and n_2 of fused silica have also shown that no resonance has been found at the wavelengths of 1064, 532, and 355 nm.[19] Hence it can be assumed that the magnitude of $\chi^{(3)}$ is constant and that the phase is nearly zero in the spectral range of interest for fused silica, ideal conditions for a reference material.

4. EXPERIMENT

A Spectra-Physics (GCR-4) *Q*-switched, injection-seeded, Nd:YAG laser generates 1064-nm optical pulses of 10-nsec FWHM at a 10-Hz repetition rate. A KDP crystal (type II phase match) is used to produce highly efficient second-harmonic radiation at 532 nm, which subsequently pumps a Spectra-Physics PDL-3 dye laser. The dye laser is tunable from 700 to 960 nm by use of visible–IR dyes. To obtain fundamental wavelengths between 900 and 1600 nm, we used a Raman shifter filled with compressed hydrogen gas whose molecular vibrational Raman mode at 4155 cm^{-1} causes stimulated Raman gain in the Stokes-shifted frequencies. The first or second Stokes-shifted frequencies from the Raman cell pumped by the Nd:YAG or dye laser are used as a fundamental input. Beyond 1600 nm a $LiIO_3$ wave mixer ($\omega_{out} = \omega_{dye} - \omega_{1064}$) is required.

The input laser beams are made TE polarized and weakly focused onto the sample so that the Rayleigh range is larger than the sample thickness for the plane-wave approximation to be valid. The sample was placed in a vacuum ($\sim 10^{-3}$-Torr) container to eliminate the THG or NDFWM contribution from air within the Rayleigh range. The thickness of the fused-silica substrate was chosen to be smaller than all the coherence lengths in the

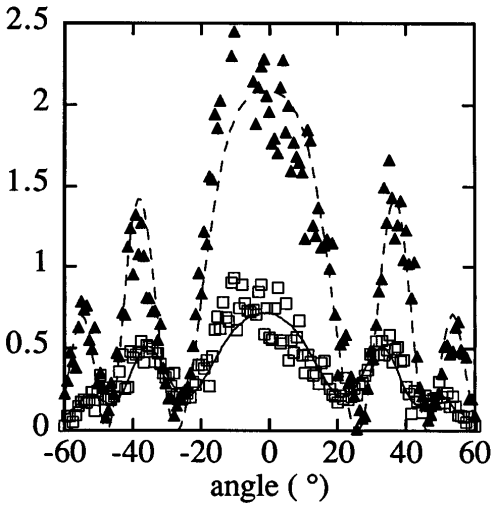

Fig. 4. Typical Maker fringe for NDFWM with $\lambda_1 = 820$ nm and $\lambda_2 = 1064$ nm. Filled triangles, substrate alone; open squares, film + substrate. Solid and dashed curves are fits to the respective data sets.

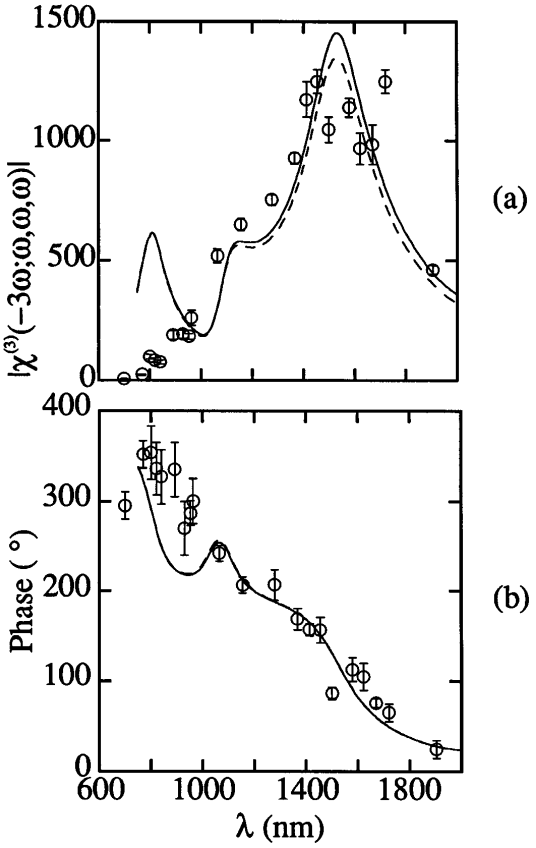

Fig. 5. (a) Magnitude and (b) phase of $\chi^{(3)}(-3\omega;\ \omega,\ \omega,\ \omega)$ versus λ. Solid curves, original four-level model; dashed curves, four-level model + Raman state.

frequency range of interest. This permitted sufficient modulation in the Maker fringes over practical angles of sample rotation. The output signal was filtered from the copropagating fundamental(s) by a combination of color filters, optical bandpass filters (Fabry–Perot type), and a monochromator. A photomultiplier tube with a preamplifier linearly converted the signal optical pulse energy into an electric current pulse that was proportional to the signal optical pulse energy. This signal was integrated by a boxcar averager, digitized, and stored in a PC that controlled the data acquisition and the rotation motor, synchronously with the 10-Hz Q-switch trigger from the Nd:YAG source.

The THG spectra shown in Fig. 5 are taken partially from Ref. 10, augmented here by additional data extended to shorter wavelengths ($\lambda < 1\ \mu$m) to probe the two-photon state near 3.1 eV predicted by Guo *et al.*[11]

The spectra of the magnitude and the phase of $\chi^{(3)}(-\omega_3;\ \omega_1,\ \omega_1,\ -\omega_2)$ obtained from the Maker fringe analysis are plotted versus λ_1 in Figs. 6 and 7 for $\lambda_2 = 1064$ nm and $\lambda_2 = 1907$ nm, respectively. At some wavelengths we repeated the measurements with different input intensities to verify that indeed there are negligible contributions from higher-order processes, in particular excited-state populations, under the present experimental conditions for both THG and NDFWM.

First, we compared the four-level model that had been used to fit the THG spectra previously with the extended THG data and the two new NDFWM spectra without changing any of the parameters used previously.[11] The energy difference between the ground state and the $1B_u$ state was fixed at 2.43 eV (510 nm). This was somewhat shifted from the measured linear absorption peak at 480 nm (Fig. 2) to account for the red shifts observed in the THG spectra. The inclusion of vibrational states could partially explain this red shift without artificially shifting the $1B_u$ state (labeled 1), as demonstrated recently in the case of the dialkyl-aminonitrostilbene (DANS) molecule.[20] The locations of the nB_u (3) and mA_g (2) states were free variables, subject to the constraint that $E_{30} > E_{20} > E_{10}$. Existence of a strong two-photon state located above the $1B_u$ state is supported by recent Kerr ellipsometry studies of a poly(3-octylthiophene) solution and two-photon fluorescence spectroscopy of a poly(p-phenylenevinylene) film, even though they are slightly different materials from PT14.[21,22] Also fixed by the model were the transition dipole moments μ_{23} and μ_{12}. μ_{03} was a free variable.[11] The fit parameters are summarized in Table 1. The previous best fit to the THG data (for $\lambda < 1\ \mu$m) shown in Fig. 5 gave $\mu_{03} \approx 0.12$ normalized to $\mu_{01} = 1$ and $\Gamma = 0.37$ eV (3000 cm^{-1}). The resulting fit to the four-level model is very good, except in the short-wavelength range.[11] However, the extended THG magnitude spectrum (for $\lambda < 1\ \mu$m) shows no strong evidence of the calculated two-photon resonance in the 800-nm (1.55-eV) range associated with an mA_g state at 3.1 eV. A two-photon excited fluorescence experiment has been performed on a thiophene oligomer, showing that an intense two-photon state is located at 2.27 eV, which is 0.11 eV above the

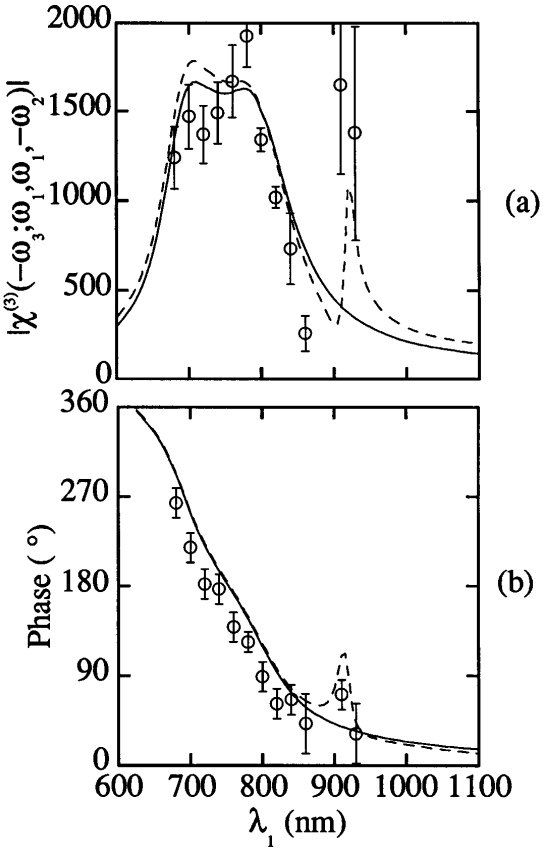

Fig. 6. (a) Magnitude and (b) phase of $\chi^{(3)}(-\omega_3;\ \omega_1,\ \omega_1,\ -\omega_2)$ versus λ_1 with $\lambda_2 = 1064$ nm. Solid curves, original four-level model; dashed curves, four-level model + Raman state.

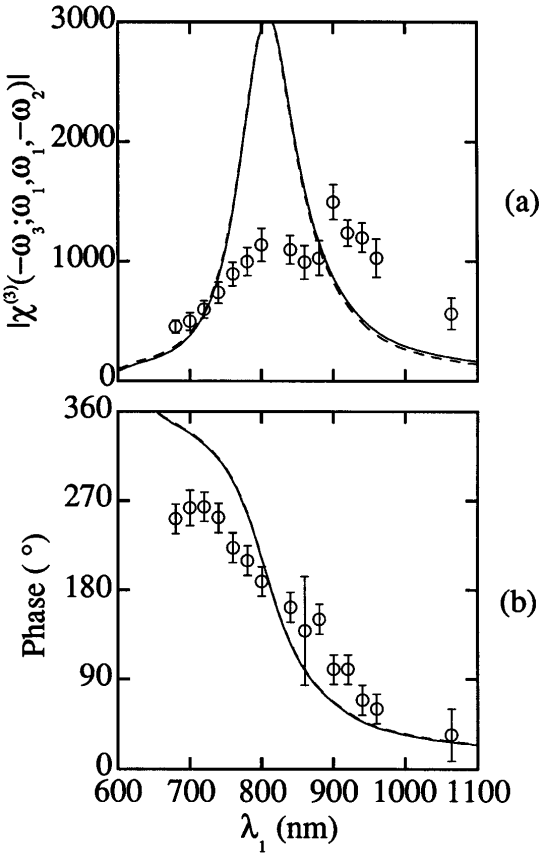

Fig. 7. (a) Magnitude and (b) phase of $\chi^{(3)}(-\omega_3; \omega_1, \omega_1, -\omega_2)$ versus λ_1 with $\lambda_2 = 1907$ nm. Solid curves, original four-level model; dashed curves, four-level model + Raman state.

$1B_u$ state.[23] Although assuming that such a two-photon state close to the $1B_u$ state can improve the fit to the THG spectra, the same parameters did not yield a reasonable fit to the NDFWM spectra.

An example of NDFWM Maker fringes is shown in Fig. 4. The signal from the substrate alone was larger than that from the film + substrate, in contrast to the THG Maker fringes.[24] This occurs when signals from the two media tend to cancel each other because of the relative phase of these materials with the particular combination of input and output wavelengths. The calculated and experimental NDFWM spectra are plotted in Figs. 6 and 7; the same parameter set as established by the THG fit, except for magnitude scaling factors, was used. No attempt was made to evaluate the absolute $\chi^{(3)}$ values for the polythiophene films because of the uncertainty involved in the current $\chi^{(3)}$ values of the fused silica. However, the scaling factors in the two NDFWM calculations were kept the same. We determined the error bars in Figs. 6 and 7 by assuming that the input laser pulse energies (or intensity) fluctuate by ±7% between the two consecutive measurements (film + substrate and substrate only) and then refitting the Maker fringes for the film + substrate, using 110% and 90% of the $\chi^{(3)}$ values obtained from fitting the substrate data according to the assumed laser energy fluctuation.

For the NDFWM with $\lambda_2 = 1064$ nm the calculated spectra are in good agreement with the experimental data (both the magnitude and the phase) for $\lambda_1 < 900$ nm, as shown in Fig. 6. It appears that the main broad peak in the magnitude spectrum consists of two overlapping resonances: the ω_3 resonance involving the $1B_u$ state ($\lambda_3 = 510$ nm or $\lambda_1 = 690$ nm) and the two-photon resonance for the mA_g state ($\lambda_1/2 = 400$ nm). Note that this two-photon resonance is necessary to explain the NDFWM data, although it did not appear clearly in the THG magnitude spectrum.

Another interesting feature in the measured NDFWM spectra in Fig. 6(a) is the peak in the 920-nm range. It cannot be an ω_3 resonance because it falls in the linear transparency region for $\lambda_1 \sim 920$ nm. Its origin could be either a two-photon or a Raman resonance. Because a two-photon peak with a narrow linewidth was not found at the same wavelength in the THG spectrum, it could be interpreted as a Raman resonance at 0.18 eV (1450 cm^{-1}), corresponding to one of the ring stretching modes of the 3-substituted thiophenes.[25] The Raman state was quantitatively included in expressions (1)–(3) as a low-lying two-photon level with a very narrow linewidth (100 cm^{-1}) and with an effective transition dipole moment of 0.5 μ_{01}, as shown in Table 1. The resulting spectra are plotted as dotted curves in Figs. 5–7. The inclusion of a Raman state explains not only the sharp peak in Fig. 6(a) but also the small narrow maximum in the phase spectrum in Fig. 6(b) without affecting the main spectral features that are due to the electronic transitions in all the nonlinear-optical spectra. Actually, in the THG and the other NDFWM ($\lambda_2 = 1907$ nm) spectra the calculated results for the original four-level model and the Raman-augmented five-level model effectively overlap, i.e., there is negligible contribution from the Raman level over the wavelength range studied.

For NDFWM with $\lambda_2 = 1907$ nm the four-level model plot does not agree well with the experimental data. The calculated magnitude spectrum predicts that two strong resonances, the ω_3 resonance associated with the $1B_u$ state and the two-photon resonance for the mA_g state, completely overlap at $\lambda_1 = 810$ nm, whereas the experi-

Table 1. Fit Parameters (Locations of Excited States and Transition Dipole Moments between Them) Used in the Four-Level Model

Energy Levels	Location (eV)	Energy Levels				
		0 ($1A_g$)	1 ($1B_u$)	2 (mA_g)	3 (nB_u)	4 (Raman)
0 ($1A_g$)	0	0	1	0	0.12	0
1 ($1B_u$)	2.43	1	0	2.2	0	0.5
2 (mA_g)	3.08	0	2.2	0	−2.0	0
3 (nB_u)	3.38	0.12	0	−2.0	0	0
4 (Raman)	0.18	0	0.5	0	0	0

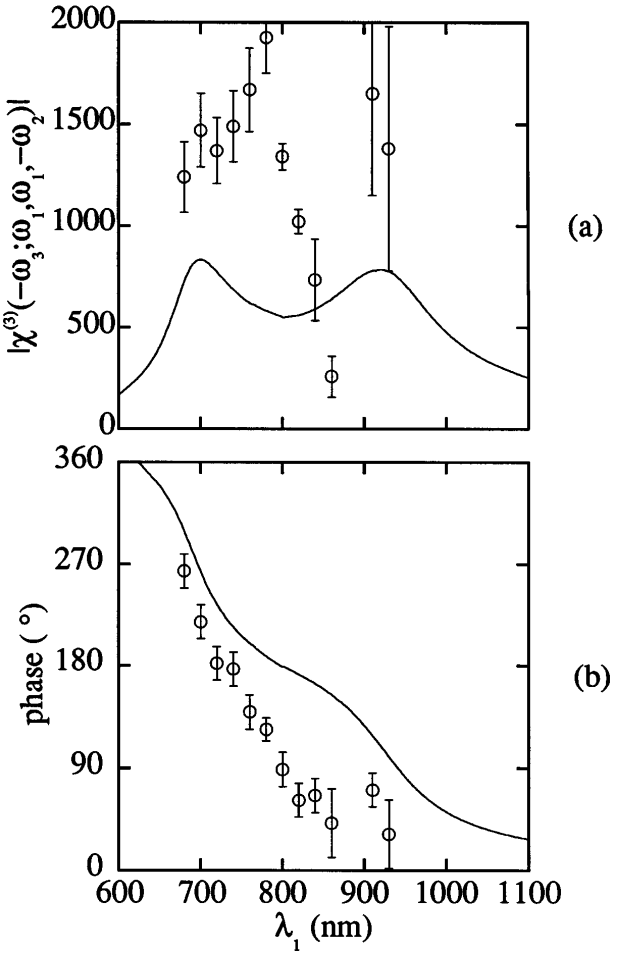

Fig. 8. (a) Magnitude and (b) phase of $\chi^{(3)}(-\omega_3; \omega_1, \omega_1, -\omega_2)$ versus λ_1 with $\lambda_2 = 1064$ nm. Solid curves, four-level model with mA_g state at 2.67 eV.

mental data show that they are close but still separated. The phase spectrum supports this conclusion. The rapid phase change from 0 to 2π in the calculated curve indicates that two resonances are concentrated near 800 nm, while the data show a slower change. One could assign the two-photon state to be at 2.67 eV (465 nm) instead of at 3.10 eV (400 nm) to fit this particular spectrum. In this case, however, the shifted two-photon state does not satisfy the other NDFWM (with $\lambda_2 = 1064$ nm) spectrum, as shown in Fig. 8.

5. CONCLUSION

We have measured the wavelength dispersion of the cubic susceptibilities of polythiophene thin films, using THG and NDFWM. The experimental spectra were compared with the calculated spectra from the four-level excited-state model whose parameters were determined previously.[11] In all three complex spectra a strong and broad three-photon resonance was present, making the deconvolution with additional multiphoton resonances difficult. It was proved that the four-level excited-state model could not fit all the spectra with a unique set of molecular parameters. A rigorous calculation based on the structures of thiophene oligomers with the addition of vibrational effects seems to be necessary to explain the nonlinear-optical spectra. We speculate that the inclusion of the contribution from the vibrational substates could have partially reduced some of the discrepancies between theory and experiments.[20] Introducing a Raman resonance improved the fit to the NDFWM spectra with $\lambda_2 = 1064$ nm without affecting the main features that were due to the electronic transitions in all the other nonlinear-optical spectra. A more rigorous molecular calculation is desirable, starting from the specific molecular structure and including more-involved configuration interactions. Experimentally the THG and NDFWM methods used were both complementary and necessary for a stringent test of current theory. To determine the locations of two-photon states exactly, direct TPA measurements are desirable in addition to the frequency-mixing experiments reported here.

ACKNOWLEDGMENT

This research was supported by U.S. Air Force Office of Scientific Research grant AFOSR (91-0339) and a strategic grant (STR0100950) from the National Science and Engineering Research Council of Canada.

REFERENCES

1. P. N. Prasad and D. J. Williams, *Introduction to Nonlinear Optical Effects in Molecules & Polymers* (Wiley, New York, 1991).
2. F. Kajzar, J. Messier, C. Sentein, R. L. Elsenbaumer, and G. G. Miller, Proc. Soc. Photo-Opt. Instrum. Eng. **1147,** 36 (1989).
3. D. Neher, A. Wolf, M. Leclerc, A. Kaltbeitzel, C. Bubeck, and G. Wegner, Synth. Metals **37,** 249 (1990).
4. T. Sugiyama, T. Wada, and H. Sasabe, Synth. Metals **28,** 323 (1989).
5. F. Kajzar, G. Ruani, C. Taliani, and R. Zamboni, Synth. Metals **37,** 1178 (1990).
6. T.-M. Lee, S. Mittler-Neher, D. Neher, G. I. Stegeman, C. Roux, M. Leclerc, J. Martin, and S. I. Najafi, Opt. Mater. **1,** 65 (1992).
7. P. B. Logsdon, J. Pfleger, and P. N. Prasad, Synth. Metals **26,** 369 (1988).
8. R. Dorsinville, L. Yang, R. R. Alfano, R. Zamboni, R. Danieli, G. Ruani, and C. Talini, Opt. Lett. **14,** 1321 (1989).
9. L. Yang, R. Dorsinville, Q. Z. Wang, W. K. Zou, P. P. Ho, N. L. Yang, R. R. Alfano, R. Zamboni, R. Danieli, G. Ruani, and C. Taliani, J. Opt. Soc. Am. B **6,** 277 (1989).
10. W. E. Torruellas, D. Neher, R. Zanoni, G. I. Stegeman, F. Kajzar, and M. Leclerc, Chem. Phys. Lett. **175,** 11 (1990).
11. D. Guo, S. Mazumdar, G. I. Stegeman, M. Cha, D. Neher, S. Aramaki, W. E. Torruellas, and R. Zanoni, Mater. Res. Soc. Symp. Proc. **247,** 151 (1992).
12. R. L. Elsenbaumer, K. Y. Jen, G. G. Miller, and L. W. Shacklette, Synth. Metals **18,** 277 (1987).
13. M. Leclerc, F. M. Diaz, and G. Wegner, Macromol. Chem. **190,** 3105 (1989).
14. B. J. Orr and J. F. Ward, Mol. Phys. **20,** 513 (1971).
15. F. Kajzar, J. Messier, and C. Rosilio, J. Appl. Phys. **60,** 3040 (1986).
16. N. Bloembergen and P. S. Pershan, Phys. Rev. **128,** 606 (1962).
17. D. Neher, A. Wolf, C. Bubeck, and G. Wegner, Chem. Phys. Lett. **163,** 116 (1989).
18. D. S. Bethune, J. Opt. Soc. Am. B **6,** 910 (1989).
19. J. R. DeSalvo, "On nonlinear refraction and two-photon absorption in optical media," Ph.D. dissertation (University of Central Florida, Orlando, Fla., 1993), p. 96.
20. D. Beljonne, J. L. Brédas, M. Cha, W. E. Torruellas, G. I. Stegeman, W. H. G. Horsthuis, and G. R. Möhlman, "Two-photon absorption and third-harmonic generation of dialkyl-

amino-nitrostilbene (DANS): a joint experimental and theoretical study," submitted to J. Chem. Phys.
21. N. Pfeffer, P. Raimond, F. Charra, and J-M. Nunzi, Chem. Phys. Lett. **201,** 357 (1993).
22. C. J. Baker, O. M. Gelsen, and D. D. C. Bradley, Chem. Phys. Lett. **201,** 127 (1993).
23. N. Periasamy, R. Danieli, G. Ruani, R. Zamboni, and C. Taliani, Phys. Rev. Lett. **68,** 919 (1992).
24. W. E. Torruellas, R. Zanoni, M. B. Marques, G. I. Stegeman, G. R. Möhlmann, E. W. P. Erdhuisen, and W. H. G. Horsthuis, Chem. Phys. Lett. **175,** 267 (1993).
25. N. B. Colthup, L. H. Daly, and S. E. Wiberley, *Introduction to Infrared and Raman Spectroscopy*, 3rd ed. (Academic, Orlando, Fla., 1990).